JACS
JOURNAL OF THE AMERICAN CHEMICAL SOCIETY
Article
pubs.acs.org/JACS
Terms of Use

Thermodynamic Mechanism for the Evasion of Antibody Neutralization in Flaviviruses

Rodrigo A. Maillard,[*,†,#] Tong Liu,[†,§] David W. C. Beasley,[‡,∥,⊥] Alan D. T. Barrett,[§,∥,⊥] Vincent J. Hilser,[†,#,▽] and J. Ching Lee[*,†,∥,⊥,#]

[†]Department of Biochemistry & Molecular Biology, [‡]Department of Microbiology & Immunology, [§]Department of Pathology, [∥]Sealy Center for Vaccine Development, [⊥]Institute for Human Infections and Immunity and [#]Sealy Center for Structural Biology and Molecular Biophysics, The University of Texas Medical Branch, Galveston, Texas 77555, United States

ABSTRACT: Mutations in the epitopes of antigenic proteins can confer viral resistance to antibody-mediated neutralization. However, the fundamental properties that characterize epitope residues and how mutations affect antibody binding to alter virus susceptibility to neutralization remain largely unknown. To address these questions, we used an ensemble-based algorithm to characterize the effects of mutations on the thermodynamics of protein conformational fluctuations. We applied this method to the envelope protein domain III (ED3) of two medically important flaviviruses: West Nile and dengue 2. We determined an intimate relationship between the susceptibility of a residue to thermodynamic perturbations and epitope location. This relationship allows the successful identification of the primary epitopes in each ED3, despite their high sequence and structural similarity. Mutations that allow the ED3 to evade detection by the antibody either increase or decrease conformational fluctuations of the epitopes through local effects or long-range interactions. Spatially distant interactions originate in the redistribution of conformations of the ED3 ensembles, not through a mechanically connected array of contiguous amino acids. These results reconcile previous observations of evasion of neutralization by mutations at a distance from the epitopes. Finally, we established a quantitative correlation between subtle changes in the conformational fluctuations of the epitope and large defects in antibody binding affinity. This correlation suggests that mutations that allow viral growth, while reducing neutralization, do not generate significant structural changes and underscores the importance of protein fluctuations and long-range interactions in the mechanism of antibody-mediated neutralization resistance.

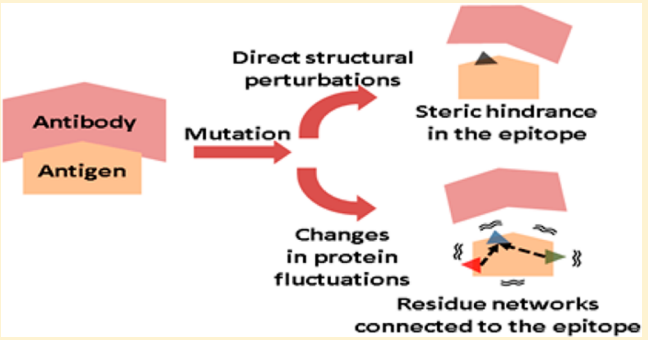

INTRODUCTION

Infectious diseases caused by flaviviruses are major concerns in the public health community, particularly those that are drug-resistant or resistant to antibody-mediated neutralization. However, the basic mechanism by which mutations in antigenic proteins lead to evasion of antibody neutralization is still unclear. In flaviviruses, the envelope protein domain III (ED3) harbors many of the critical mutations that have been shown to reduce antibody neutralization.[1−9] The ED3 forms a classic β-sandwich fold that is conserved among flaviviruses (Figure 1A, side view). The N-terminus and loops connecting β-strands B−C, D−E, and F−G form a surface patch that is exposed to the solvent in the viral particle (Figure 1A, top view).[10−16] Structural studies have shown that effective neutralizing monoclonal antibodies (mAbs) recognize this surface patch with a high degree of shape complementarity.[12,17,18]

Interestingly, within the large ED3−mAb interaction surface, a few specific mutations significantly decrease mAb binding and reduce neutralization *in vivo*,[19,20] depending largely on the type of side chain substitution. In the ED3 of West Nile virus (WNV), the mutations T332K and T332M reduced mAb binding almost completely (>80% reduction compared with wild-type).[1,19−22] The mutation T332A partially reduced mAb binding (~50% reduction),[19,20] whereas T332V had no effects in antibody binding.[20] This broad spectrum of mutational effects on mAb binding is also observed in the ED3s of other flaviviruses, such as mutations at positions S331 and D332 in Japanese encephalitis virus (JEV),[23] a serologically close relative of WNV, or mutations at positions K305 and K307 in dengue virus type 2 (DENV-2),[24] a distant relative of WNV and JEV.

Moreover, not only mutations within the interaction surface itself prevent mAb binding and neutralization, but mutations can occur outside the binding site and influence antibody binding via long-range effects. These observations motivated us to address the following questions: What is the nature of epitopes? What is the mechanism by which mutations outside the antigen−antibody contact region reduce mAb binding? Is there a network of interacting residues, wherein mutations perturb distantly positioned regions of the protein?

Received: April 2, 2014
Published: June 20, 2014

dx.doi.org/10.1021/ja503318x | J. Am. Chem. Soc. 2014, 136, 10315−10324

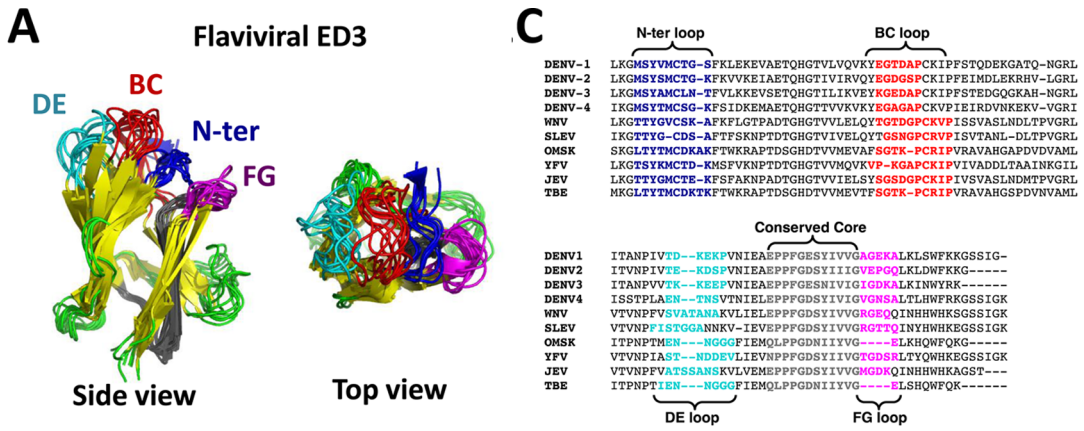

B

Root mean square deviation between all atoms (in Angstroms)										
Virus	DENV 1	DENV 2	DENV 3	DENV 4	WN V	STLEV	OMSK	YFV	JEV	TBEV
Dengue 1										
Dengue 2	1.0									
Dengue 3	1.0	0.8								
Dengue 4	1.4	1.2	1.5							
West Nile virus	2.6	2.5	2.4	2.6						
St. Louis Encephalitis	1.3	1.2	1.4	1.6	2.4					
Omsk	2.0	1.5	1.9	1.9	2.6	1.8				
Yellow Fever	2.2	2.0	2.2	2.4	2.4	1.8	2.8			
Japanese Encephalitis	2.6	2.4	2.4	2.8	2.6	2.4	2.7	3.8		
Tick-borne encephalitis	1.4	1.0	1.4	1.5	2.3	1.4	0.9	2.3	2.1	

Figure 1. Structural and sequence analysis of the ED3 from different flaviviruses. Structural alignment of the ED3 from different flaviviruses: dengue virus types 1, 2, 3 and 4, DENV-1 (PDB 3IRC), DENV-2 (PDB 1TG8), DENV-3 (PDB 1UZG), and DENV-4 (PDB 2H0P), respectively; West Nile virus, WNV (PDB 1S6N); St. Louis encephalitis virus, SLEV (PDB 4FG0); Omsk hemorrhagic fever, OMSK (PDB 1Z3R); yellow fever virus, YFV (PDB 2JQM); Japanese encephalitis virus, JEV (PDB 1PJW); tick-borne encephalitis, TBE (PDB 1SVB). The rmsd (all atoms) among all ED3 structures is between 1 and 4 Å. β-Strands are colored in yellow, random coils are colored in green, and a highly conserved hydrophobic core found in most flaviviruses is colored in gray. The loops DE (cyan), BC (red), N-terminus (blue), and FG (pink) form a patch of residues that are exposed to the solvent in the context of the intact viral particle.[10,11] The figures were rendered using PyMOL v. 0.97 (Delano Scientific LLC, San Carlos, CA). The sequence alignment shows the amino acids of each solvent-exposed loop and the conserved hydrophobic core.

Addressing these questions using high-resolution structures and antibody binding data is challenging and time-consuming, particularly for phylogenetically and serologically related viruses whose protein antigens typically share a high degree of structural and sequence similarity. The structures of the ED3 of various flaviviruses, shown in Figure 1A, are very similar, making it difficult to identify specific features in each viral protein that may be associated with unique antigenicity. Hence, an alternative approach is needed, and the ED3 of flaviviruses was adopted as a model system. Based on increasing experimental evidence highlighting the importance of protein conformational fluctuations in biological function,[25] we hypothesized that epitopes are intrinsically encoded in the thermodynamic properties of the conformational fluctuations of the ED3s. Thus, even if the protein antigens look alike, their thermodynamic properties might differ significantly.

To test our hypothesis, we investigated whether mAb-resistant mutations affect the conformational fluctuations in the ED3s of two related but serologically distinct flaviviruses, WNV and DENV-2. In this study, we used an algorithm that allowed us to explore the thermodynamic properties of correlated fluctuations in computer-generated protein ensembles.[26−30]

Our results support a model of evasion of antibody-mediated neutralization that involves changes in the protein's conformational fluctuations and long-range interactions between mutation sites and epitopes. This study also reveals fundamental thermodynamic properties of residues residing in epitopes that may have general implications for other pathogens.

METHODS

Generation of a Conformational Ensemble around the Native Structure. To investigate the thermodynamic properties of protein fluctuations in the ED3s from WNV and DENV-2, we used the COREX algorithm.[26,27] Briefly, COREX generates a native state ensemble from the target protein structure (PDB 1S6N for WNV and 1TG8 for DENV-2) through the combined unfolding of adjacent groups of residues defined as folding units. Folding units are treated as native-like or as unfolded peptides. Within this ensemble, the free energy of each conformational state, ΔG_i, is calculated with a surface-area parametrization that has been validated experimentally.[26,27] By rewriting ΔG_i as an equilibrium constant (K_i) between the conformer i and the folded state ($K_i = \exp[-\Delta G_i/(RT)]$), we define the probability (P_i) of each conformer as

$$P_i = \frac{K_i}{\sum_i K_i} = \frac{K_i}{Q} \tag{1}$$

In eq 1, Q is the sum of all possible states in the ensemble (partition function). Moreover, ΔG_i can be resolved into the energetic contributions from each residue in the protein: $\Delta G_i = \sum_j^{N=aa} \Delta G_{ij}$, which allows the investigation of thermodynamic properties at the residue level.[25]

Residue Stability in the Ensemble of the ED3s. Within the ED3 ensembles, we estimated the relative stability of each residue, $\Delta G_{f,j}$, as the ratio of the probability that residue j is in the folded state ($P_{f,j}$) to the probability that the same residue is in the unfolded state ($P_{u,j}$):

$$\Delta G_{f,j} = -RT \ln(\kappa_{f,j}) = -RT \ln\left[\frac{P_{f,j}}{P_{u,j}}\right] \tag{2}$$

From eq 2, residues with high stability are mostly in the folded state in the ensemble, whereas residues with low stability are mostly in the unfolded state.

Characterization of the Long-Range Interactions in the ED3 Ensemble. We describe pairwise residue interactions in the ED3s as the thermodynamic coupling between two residues j and k.[28,29] The first step to obtain a quantitative value of the thermodynamic coupling is to evaluate the effect of an energetic perturbation on residue k ($=\Delta g^{pert,k}$) over the stability of residue j. This is accomplished by recasting eq 2 to consider the folding state of a second residue k. After rewriting eq 2, we evaluated the effect of $\Delta g^{pert,k}$ over the stability constant of residue j:

$$\Delta G_{f,j}^{pert,k} = -RT \ln(\kappa_{f,j}^{pert,k}) = -RT \ln\left[\frac{\varphi^{pert,k} P_{f,j|f,k} + P_{f,j|u,k}}{\varphi^{pert,k} P_{uj|f,k} + P_{u,j|u,k}}\right] \tag{3}$$

In eq 3, the modified residue stability constant ($\Delta G_{f,j}^{pert,k}$) considers the probabilities of states where residues j and k are both folded ($P_{f,j|f,k}$), both unfolded ($P_{u,j|u,k}$), or one in each state (either $P_{f,j|u,k}$ or $P_{u,j|f,k}$). Thus, an energetic perturbation on residue k ($\varphi^{pert,k} = \exp[-\Delta g^{pert,k}/(RT)]$) can have a stabilizing, a destabilizing, or no effect over residue j. This thermodynamic effect can be quantified by subtracting eq 3 from eq 2:

$$\Delta\Delta G_{f,j}^{pert,k} = \Delta G_{f,j} - \Delta G_{f,j}^{pert,k} \tag{4}$$

Importantly, this analysis does not require residues j and k to be in close proximity in the primary sequence or in the tertiary structure of the protein. Thus, the value $\Delta\Delta G_{f,j}^{pert,k}$ from eq 4 characterizes long-range effects of residue k over residue j.

Given that a long-range effect is not a bidirectional phenomenon *per se*,[28] in this study we define thermodynamic coupling as a bidirectional long-range effect. In other words, thermodynamic coupling is the sum of the influence of a perturbation on residue j over residue k ($\Delta\Delta G_{f,k}^{pert,j}$) and the reciprocal effect, namely, the influence of a perturbation on residue k over residue j ($\Delta\Delta G_{f,j}^{pert,k}$):

$$\Delta\Delta G_{j,k} = \Delta\Delta G_{f,k}^{pert,j} + \Delta\Delta G_{f,j}^{pert,k} \tag{5}$$

Thermodynamic coupling between two residues can be manifested in three ways: positive ($\Delta\Delta G_{j,k} > 0$), negative ($\Delta\Delta G_{j,k} < 0$), and neutral ($\Delta\Delta G_{j,k} = 0$).[28] Positive coupling occurs when stabilization or destabilization of the j residue stabilizes or destabilizes, respectively, the k residue. For negative coupling, the principles are the same, but the effect is opposite. Namely, stabilization of the j residue results in the destabilization of the k residue, and vice versa. Neutral coupling indicates that the two residues are not thermodynamically coupled.

Equation 5 provides a quantitative descriptor for long-range interactions between residues in the ED3s. With this analysis, we can investigate the long-range effects of a mutation by calculating the thermodynamic coupling between residues of mutant proteins ($\Delta\Delta G_{j,k}^{mut}$).

Response of a Boltzmann Equilibrium Process. A general Boltzmann equilibrium process, $F(x)$,[31−33] is defined as

$$F(x) = \frac{1}{1 + f(x)} = \frac{1}{1 + e^{-C(x_o - x)/(RT)}} \tag{6}$$

In eq 6, $f(x)$ is the Boltzmann factor, x corresponds to the thermodynamic coupling ($\Delta\Delta G_{j,k}$), x_o is the midpoint of the transition between the two states, and C is a cooperativity constant that describes the sharpness of the transition. The response of a Boltzmann equilibrium process is mathematically obtained by taking the derivative of eq 6 with respect to x:

$$F'(x) = \frac{d}{dx}\left[\frac{1}{1 + f(x)}\right] = \frac{C}{RT}\frac{f(x)}{[1 + f(x)]^2} \tag{7}$$

$F'(x)$ is a peaked function that describes the relationship between ΔG_{mAb} and thermodynamic coupling ($\Delta\Delta G_{j,k}$) shown in Figure 6.

Measurement of Antibody Binding to ED3s. We measured antibody binding to the ED3 from WNV wild-type and the single-site mutants E390D, H396Y, L312V, V371I, V338I, and L375I against three type-specific MAbs, 5H10, 5C5, and 3A3 (Bioreliance Corp., Rockville, MD), using published protocols.[21] Binding data for other single-site mutant ED3s from WNV or DENV-2 used in this study were obtained from the literature (Table 1).

RESULTS

Thermodynamic Signatures Encoded in the Epitopes of the ED3s. To obtain thermodynamic information for the ED3s, we used a computer algorithm to generate an ensemble of conformational states around the native structure.[27] This algorithm models fluctuations in proteins as simultaneous local unfolding reactions throughout the structure of the target protein (see Methods). After generating more than 10^6 conformational states of the ED3s, we sought to determine whether the ensemble could reveal virus-specific epitopes. We applied the ensemble model to the ED3 from WNV and DENV-2. Their root-mean-square deviation (rmsd) between all atoms is 2.5 Å (Figures 1B), and their sequence similarity is ∼50% (Figure 1C). Hence, these ED3s have high structural similarity and share high sequence identity.

Differences in Epitopes. The differential effect of mutations in resistance to antibody-mediated neutralization and their limited antigenic relatedness, indicate that the primary epitopes in WNV and DENV-2 are distinct. Our previous studies using

Table 1. Thermodynamic Coupling and Binding Affinities of Single-Site Mutants in the ED3s from DENV-2 and WNV

	mAb affinity ($K_{d,app}$, nM)	thermodynamic coupling[c] (kcal/mol)
	DENV-2[a]	
K388G	11.7	1.58
K305G	108.0	1.73
E383G	80.0	1.78
wild-type	3.81	2.01
I379V	4.67	2.19
K393R	5.42	2.26
K334Q	3.68	2.36
R345K	4.34	2.38
S331A	4.38	2.42
D329G	14.2	2.43
E327G	13.3	2.44
K307G	13.8	2.49
P384N	>80	2.56
P384D	>100	2.65
	WNV[b]	
K307R	11	1.96
K307E	8.0	2.00
Y329K	12.2	2.03
Y329F	11.6	2.02
wild-type	0.17	2.24
A365S	0.18	2.35
L312A	0.17	2.44
A369S	0.17	2.45
E390D	0.41	2.46
H395Y	0.20	2.47
L312V	0.17	2.49
V371I	0.09	2.49
K310T	0.39	2.47
V338I	0.47	2.50
L375I	0.22	2.50
T330I	7.5	2.64
T332A	1.03	2.86
T332K	10.7	2.97

[a]Binding data for the ED3 from DENV-2 against two type-specific MAbs, 5H5 and 9F16, was obtained from Hiramatsu et al.,[36] Gromowski and Barrett,[24] and Pitcher et al.[51] [b]For the WNV ED3s K307R, K307E, Y329K, Y329F, wild-type, A365S, L312A, A369S, K310T, T330I, T332A, and T332K, binding data against type-specific MAbs 5H10, 5C5, and 3A3 was obtained with permission from Beasley and Barrett,[1] Volk et al.,[13] Li et al.,[19] Maillard et al.,[21] and Zhang et al.[9] For the WNV-ED3s E390D, H396Y, L312V, V371I, V338I, and L375I, we measured mAb binding against the same three type-specific MAbs. For each mAb, binding was measured in triplicate. The error in K_d was less than 15%. [c]Mean thermodynamic coupling of residues in the BC loop (328−338) for WNV and in the FG loop (378−388) for DENV-2.

virus-specific neutralizing antibodies show that mutations at residue T332 generate a resistant phenotype in WNV,[1,9,20,22,34] whereas mutations at the homologous position in the ED3 from DENV-2, residue S331, have no significant effect. Conversely, mutations in position K310 in the ED3 from WNV do not generate a resistance phenotype in the virus, whereas mutations in the homologous position in DENV-2 do (residue K307) (Figure 2A). For example, relative to the wild-type proteins, the mutation T332A in the ED3 from WNV decreased antibody binding energy by ∼10% (equivalent to a reduction in K_d of 5-fold), whereas the mutation S331A in

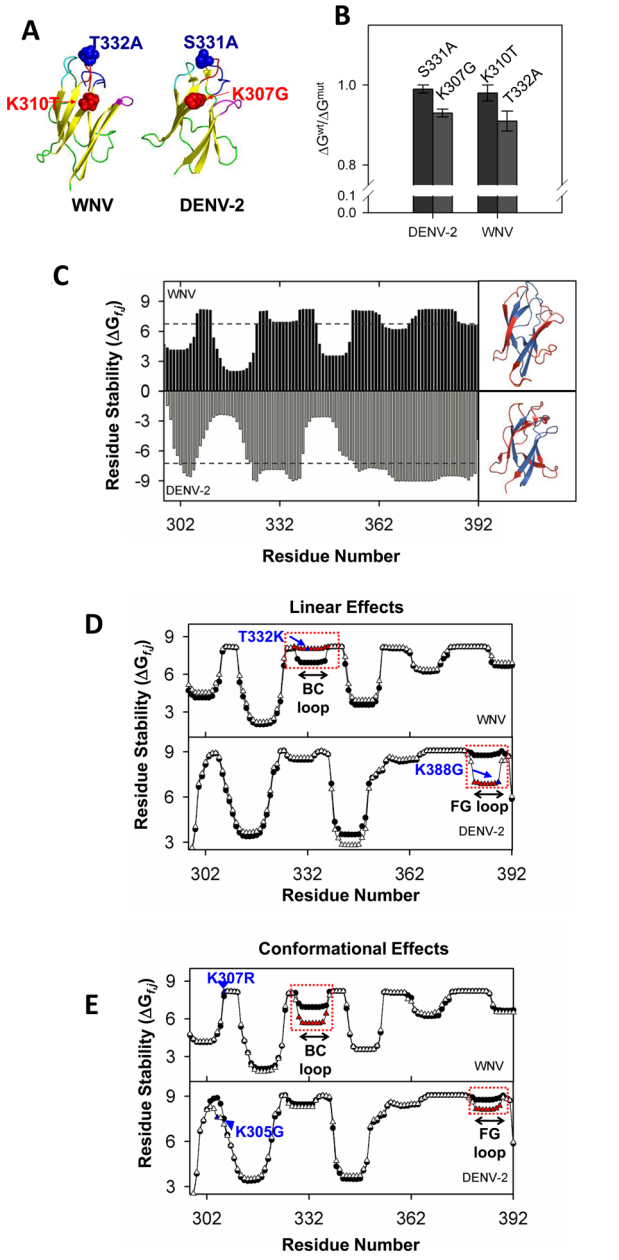

Figure 2. Thermodynamic properties in the ED3 reveal epitope location. (A) Single-site mutations at homologous positions in the ED3 from DENV-2 and WNV. Mutation S331A in DENV-2 and mutation T332A in WNV are located in the BC loop. Mutations K307G and K307T in DENV-2 and WNV, respectively, are located in the N-terminal loop. (B) Effect of the mutations shown in part A on the binding energy to type-specific MAbs.[1,24] The vertical axis is the ratio of binding energies between mutant and wild-type ED3s. (C) Residue stability plots ($\Delta G_{f,j}$) of the ED3s from WNV (top) and DENV-2 (bottom). The residue stabilities for DENV-2 were plotted as $-\Delta G_{f,j}$. The dashed line represents a threshold that separates residues with low and high stability. This threshold was obtained by considering the ∼20% lowest stability from the residue stability distribution. Residues with high stability (blue) are mostly located in the core of the protein, whereas residues with low stability (red) are solvent exposed. (D) Linear effect of mutations on the residue stability of the ED3s from WNV and DENV-2. The top panel shows the residue stability plot of the wild-type ED3 from WNV (●) and the resistant mutation T332K (△). The amino acids perturbed by the mutation correspond to residues in the BC loop (red, dotted square). The bottom panel shows the residue stability plot for the wild-type ED3 (●) and the

dx.doi.org/10.1021/ja503318x | J. Am. Chem. Soc. 2014, 136, 10315−10324

Figure 2. continued

resistant mutant K388G from DENV-2 (△). The effect of the mutation is concentrated to residues in the FG loop (red, dotted square). (E) Conformational effects on the stability constant of WNV and DENV-2. The top panel displays the destabilizing effect of the mutation K307R (blue arrowhead) in WNV. The affected residues due to the K307R mutation correspond to the BC loop (red, dotted box). In contrast, the mutation K305G in DENV-2, which is located in a structurally homologous position to K307 in WNV, had destabilizing effects over residues in the FG loop (bottom panel).

DENV-2 did not have any effect (Figure 2B). The mutation at position K307G in DENV-2 showed a similar reduction in binding energy and K_d, while the mutation K310T in WNV had no significant effect[1,24] (Figure 2B).

Stability of ED3 and Effects of Mutations on Stability Profiles. To test whether the differential effect of mutations between the ED3 of WNV and DENV-2 on antibody binding were due to differences in the conformational ensembles and their sensitivity to mutations, we characterized the stability (eq 2 in Methods) of each residue in the ensemble of the wild-type ED3s. Then, we determined what amino acids were thermodynamically perturbed (stabilized or destabilized) by resistant and nonresistant mutations previously described in WNV and DENV-2 (column 1 in Table 1).

The plot $\Delta G_{f,j}$ vs amino acid position of the wild-type ED3s is shown in Figure 2C. The top panel corresponds to the values of $\Delta G_{f,j}$ for WNV. The bottom panel shows the values for DENV-2, plotted as $-\Delta G_{f,j}$ to resemble a mirror image between the two residue stability profiles. This mirror image suggests that the analysis of the residue stability captures both the structural and the sequence similarities between these two protein antigens. As expected from the ED3 structures, highly stable amino acids are found in the protein cores, while those with low stability are located in solvent-exposed structures or random coils (Figure 2C, structures). Not expected, however, were the two distinct effects that resistant mutations had on the residue stability constants. The first effect was the perturbation of the stability constant of residues near the mutation sites or "linear effects". This linear effect was observed in residues 328−338 for resistant mutations in WNV such as T330I, T332A, and T332 K and (Figure 2D, top). Resistant mutations in DENV-2 such as E383G or K388G had linear effects over the stability of residues 378−388 (Figure 2D, bottom).

The second type of mutational effects was "conformational effects", wherein the effect of the resistant mutations was not localized to nearby residues in the primary sequence. For example, mutations in the N-terminal loop, such as K307R in WNV and K305G in DENV-2, destabilized residues in the BC loop (328−338) for WNV and in the FG loop (378−388) for DENV-2 (Figure 2E, top and bottom, respectively). Noteworthy, the BC and FG loops have been identified as major mAb-neutralizing epitopes in WNV and DENV-2, respectively.[1,5,9,24,35,36]

Residue Interaction Networks in the ED3s. To better understand the basis for mutational effects over the BC and FG loops, we sought to identify the thermodynamic properties of these loops that distinguish them from other structural elements in the ED3s. To address this, we determined the correlated thermodynamic fluctuations, or thermodynamic coupling, between residues in the ED3 ensembles. Thermodynamic coupling (defined as $\Delta\Delta G_{j,k}$, eq 5 in Methods) applies even if two residues are distantly positioned in the protein structure,[28,29] allowing the characterization of long-range residue networks in the ED3.

To experimentally validate the analysis of thermodynamic coupling, we compared calculated long-range mutational effects between distantly positioned residues in the ED3 from WNV with previously published experimental data.[21] Specifically, we correlated the effect of the single-site mutations K310T, T332A, and T332K on the solvent accessibility and dynamics of the single tryptophan residue W397, which is located ∼2 nm away from the mutation sites in the ED3 structure.[24] The mutations K310T, T332A, and T332K linearly increased the solvent-accessibility and dynamics of W397, which correlated very well with the linear increase of our calculated long-range mutational effects (R^2 = 0.98) (Figure 3A). The agreement between experimental and calculated data demonstrates that analysis of the thermodynamic coupling captures long-range interactions between residues in ED3. These published results

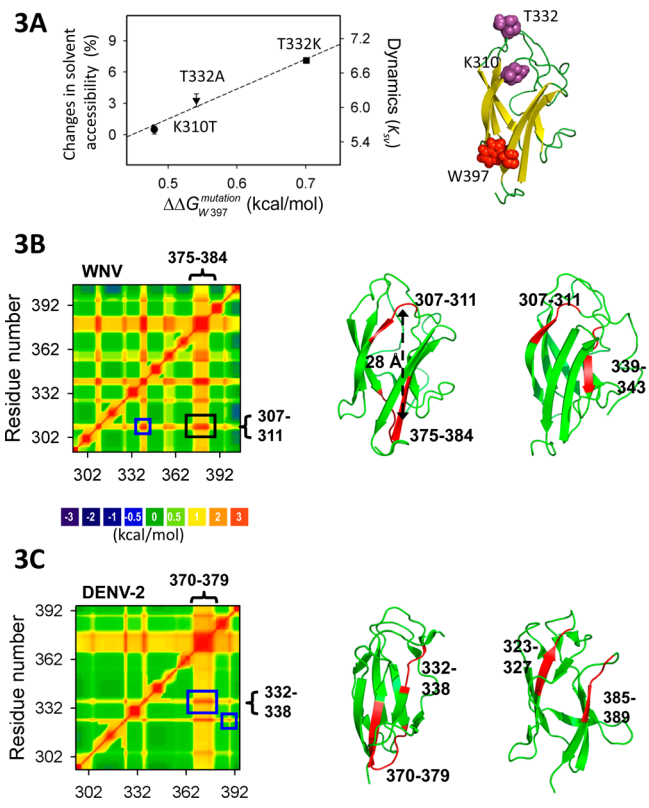

Figure 3. Residue interaction networks in the ED3 ensemble. (A) Long-range mutational effect on the solvent accessibility and protein dynamics near the single tryptophan residue in the ED3 from WNV (W397). The dynamics of the W397 residue was characterized with the Stern−Volmer quenching constant (K_{SV}). Data were obtained with permission from Maillard et al..[21] The values of $\Delta\Delta G^{mutation}_{W397}$ were calculated using eq 4 in Methods. The structure on the right side displays the position of the mutation sites and W397. (B) Thermodynamic coupling (eq 5 in Methods) between each residue pair in the ED3 from WNV. The color scaling represents the thermodynamic coupling between each residue pair, from −3 kcal/mol (purple/blue color) to 3 kcal/mol (orange/red color). Residues displaying little or no thermodynamic coupling are colored in green. The blue and black squares highlight distantly positioned residues that share high positive thermodynamic coupling. (C) Thermodynamic coupling between residue pairs in the ED3 from DENV-2. Data is rendered identically as in panel B.

dx.doi.org/10.1021/ja503318x | J. Am. Chem. Soc. 2014, 136, 10315−10324

are consistent with those from molecular dynamics simulations (Gottipati, Dodson and Lee, in preparation).

West Nile Virus. We determined the entire set of long-range interactions in the ED3 by calculating the pairwise thermodynamic coupling in the wild-type protein ($\Delta\Delta G^{wt}_{j,k}$). The plot of $\Delta\Delta G^{wt}_{j,k}$ forms an $N \times N$ matrix that describes the thermodynamic coupling at the residue level, where N is the total number of amino acids in the structure. We rendered the values of $\Delta\Delta G^{wt}_{j,k}$ in a color map (Figure 3B,C), wherein amino acids with positive thermodynamic coupling are in red, residues that manifest negative thermodynamic coupling are in blue, and residues that are not thermodynamically coupled are in green.

The results of $\Delta\Delta G^{wt}_{j,k}$ for WNV, shown in Figure 3B, reveal several features. First, the algorithm captures the expected local perturbations to nearby residues, as delineated by the positive thermodynamic coupling running in diagonal from the lower left to the upper right of Figure 3B. Second, there is positive and negative thermodynamic coupling between several groups of residues that are distantly positioned in the tertiary structure, indicating that there is a complex long-range interaction network between residues that is encoded in the native state ensemble of the ED3. Third, there appears to be a grid of high coupling that connects distal regions of the protein. Particularly pronounced among these regions are residues 375 through 384, which are thermodynamically coupled with the entire ED3. The relatively high coupling between these sites and the rest of the protein indicates a high mutual susceptibility to perturbations that will likely affect other residues. When residues 375−384 are mapped onto the ED3 structure, it is clear that they are part of a highly conserved hydrophobic core of this family of viral protein domains (Figure 1, β-strand colored in gray).

Dengue Virus 2. Similar analysis of the thermodynamic coupling in ED3 from DENV-2 also showed positive thermodynamic coupling between distant residues, as well as a conserved core of hydrophobic residues that are thermodynamically coupled with the entire protein antigen (residues 370−379) (Figure 3C). Residues 370−379 in ED3 from DENV-2 and residues 375−384 in ED3 from WNV are conserved both in sequence and in structure (Figure 1). Altogether, these analyses show that the ED3s do not behave as rigid structures but rather as conformational ensembles that are capable of transmitting long-range effects between even distant residues.

Single Mutations Are Thermodynamically Coupled to the Epitope. Against this backdrop of global coupling between core residues, we sought to determine the effect of mutations on the residue networks of the ED3s. We investigated how single-site mutations in WNV and DENV-2 perturb the pattern of thermodynamic coupling observed in the wild-type ED3s (Figure 3B,C, respectively). Our goal was to identify the unique thermodynamic features of mutations that confer resistance to antibody-mediated neutralization compared with those that do not. We analyzed the thermodynamic coupling of a panel of resistant and nonresistant mutations of WNV and DENV-2 (Table 1). For the mutants analyzed, the general pattern of thermodynamic coupling was qualitatively similar to that of the wild-type ED3s ($\Delta\Delta G^{mut}_{j,k} \approx \Delta\Delta G^{wt}_{j,k}$). The similarity between $\Delta\Delta G^{wt}_{j,k}$ and $\Delta\Delta G^{mut}_{j,k}$ for both WNV and DENV-2 (Figure 4) indicates that the overall energetic hierarchy of states (i.e., what states are most stable) of the ED3s is thermodynamically robust and that single mutations do not disrupt the basic networks of long-range interactions between residues. Despite these similarities, however, important differences were revealed by

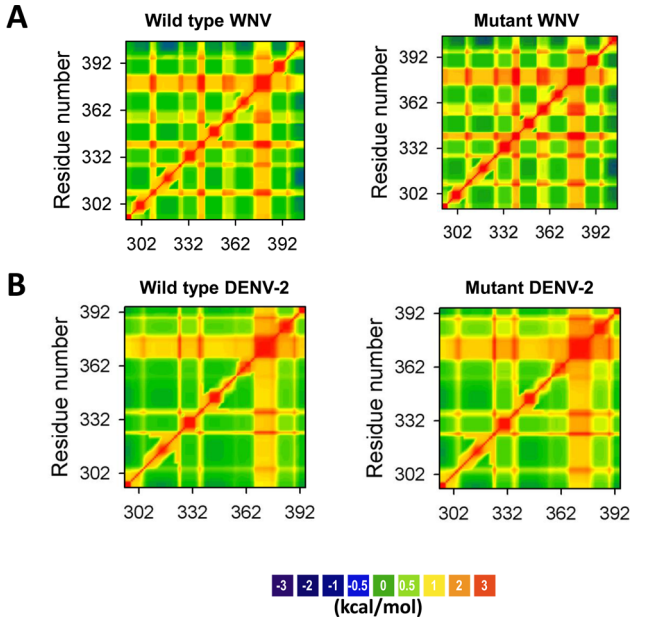

Figure 4. Thermodynamic coupling of single site mutants of the ED3 from WNV and DENV-2 (A) Thermodynamic coupling observed for the WNV wild-type ED3 and for a representative mutant. (B) Thermodynamic coupling from DENV-2 wild-type ED3 and a representative mutant.

subtracting the values of thermodynamic coupling of the wild-type ED3, $\Delta\Delta G^{wt}_{j,k}$, from those of the mutant, $\Delta\Delta G^{mut}_{j,k}$ (Figure 5). This difference, $\Delta\Delta G^{mut}_{j,k} - \Delta\Delta G^{wt}_{j,k}$, quantifies the relative impact of each mutation on the coupling network in each ED3 and reflects the response of the ensemble to a resistant or nonresistant mutation.

West Nile Virus. The plot of $\Delta\Delta G^{mut}_{j,k} - \Delta\Delta G^{wt}_{j,k}$ for resistant mutations in the ED3 from WNV revealed three striking features (Figure 5A). First, the effect of the mutation on the thermodynamic coupling was localized mainly to residues 328−338, that is, the BC loop, the major neutralizing epitope in the ED3 of WNV. Second, depending on the type and position of the mutation, we observed two distinct effects on the thermodynamic coupling of residues 328−338. Mutations at position T330 and T332 increased the magnitude of thermodynamic coupling (positive effects), while mutations at position K307 decreased the degree of thermodynamic coupling (negative effects) (Figure 5A, center and right). Third, residues 328−338 become thermodynamically coupled with the rest of the amino acids in ED3. This last observation indicates that the effect of a resistant mutation is not limited to nearby residues. Thus, the ability of a mAb to neutralize a virus can be impaired by a single mutation, even if that mutation is outside of the mAb binding site. The analysis of mutations that have no effect on mAb neutralization resistance in WNV (e.g., K310T)[1,19,21] revealed minimal changes in the thermodynamic coupling over residues 328−338 or other regions in the ED3 (Figure 5A, left).

Dengue Virus 2. The plot of $\Delta\Delta G^{mut}_{j,k} - \Delta\Delta G^{wt}_{j,k}$ for DENV-2 also revealed positive or negative effects on the thermodynamic coupling for mutations that confer resistance to neutralization (Figure 5B). However, and most interestingly, the effects of the mutations were concentrated on residues in the FG loop of the ED3 structure (residues 378−388), the major epitope in DENV-2 (Figure 5B, center and right) Remarkably, resistant

dx.doi.org/10.1021/ja503318x | J. Am. Chem. Soc. 2014, 136, 10315−10324

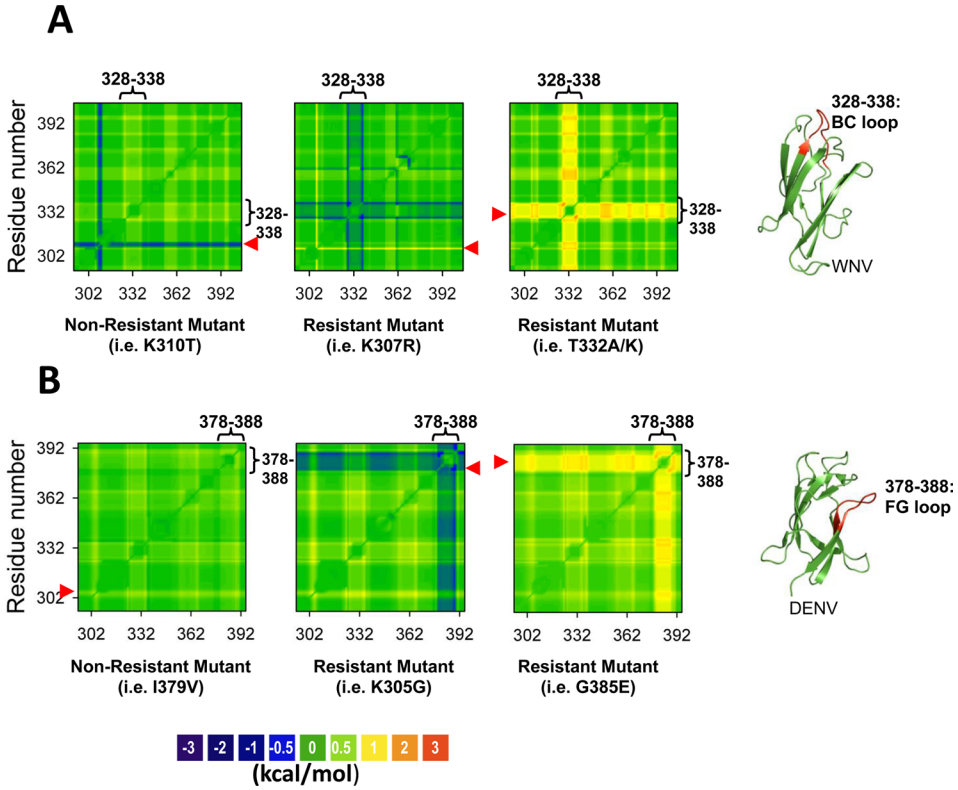

Figure 5. Antibody resistant mutations are thermodynamically coupled to the epitope. (A) Effect of mutations on the thermodynamic coupling of the ED3 from WNV. The plot corresponds to $\Delta\Delta G^{mut}_{j,k} - \Delta\Delta G^{wt}_{j,k}$. The color scale ranges ±1 kcal/mol. Resistant mutations such as K307R (middle) decreased the thermodynamic coupling of residues 328−338. The mutation T332K, another resistant mutation, increased the thermodynamic coupling of residues 328−338. Mutations that do not confer resistance against antibody neutralization, such as the K310T mutation, did not have any large effect on the thermodynamic coupling of residues 328−338. (B) Effect of mutations on the thermodynamic coupling of the ED3 from DENV-2. Resistant mutations either increased or decreased the thermodynamic coupling of residues 378−388. Nonresistant mutations such as I379V did not significantly affect any other part of the protein.

mutations such as K305G and K307G had a negative effect on the thermodynamic coupling of the FG loop despite being located outside of the affected area. Moreover, residues 378−388 became thermodynamically coupled to the rest of amino acids in ED3, underscoring again the long-range effects of the resistant mutations on the thermodynamic properties of the protein antigen.

Since the calculations in this study are based on the thermodynamics of protein fluctuations,[26,27] these results indicate that resistant mutations in ED3 change the conformational dynamics of specific loops that correspond to the primary epitopes in the protein antigens.[1,5,19,24,35] Moreover, the positive and negative coupling effects on these loops are observed exclusively in mutations that confer antibody resistance.

DISCUSSION

Identities of Epitopes Correlate with Susceptibility to Energetic Perturbations. In the present study, we used an experimentally validated ensemble model[33,34] to investigate the molecular mechanism by which single-site mutations in WNV and DENV-2 lead to evasion of antibody-mediated neutralization. Our approach successfully identified the location of the primary epitopes in the ED3s of WNV and DENV-2, despite the high structural and sequence similarity between the two protein antigens. Thus, even if two viral proteins share high sequence and structural stability, the response of the ensemble to mutations is unique. Equally important is that the ensemble-based thermodynamic analysis used in this study reveals a previously unidentified relationship between mutational susceptibility and epitope location, a relationship that could prove useful for *a priori* identification of specific primary epitopes in different viruses.

A Thermodynamic Mechanism of Resistance to Antibody-Mediated Neutralization. We observed that evasion of neutralization and decrease in mAb binding was caused by mutations that triggered changes in the conformational fluctuations of the epitopes. Based on this observation, we sought to establish a quantitative relationship between changes in the conformational fluctuations and mAb binding. To this end, for each ED3 mutant, we plotted the thermodynamic coupling of the residues in the epitope ($\Delta\Delta G_{epitope}$) and their corresponding binding energies to MAbs ($\Delta G_{mAb} = -RT \ln[K_{eq}]$, where K_{eq} is the equilibrium binding constant).

Figure 6A shows the mean thermodynamic coupling of residues in the BC loop for WNV and their respective mAb binding energies, ΔG^{WNV}_{mAb} (Figure 6A, red squares). In the same figure, we included the plot for DENV-2, but with the values of mean thermodynamic coupling of residues in the FG loop and their respective mAb binding energies, ΔG^{DENV-2}_{mAb} (Figure 6, blue circles). Qualitatively, the two plots in Figure 6A have a similar shape, following a peaked function. Moreover, Figure 6A shows that for both viruses mutations that significantly decrease the mAb binding energy (i.e., low binding constants) also exerted the largest changes in the thermodynamic coupling

dx.doi.org/10.1021/ja503318x | J. Am. Chem. Soc. 2014, 136, 10315−10324

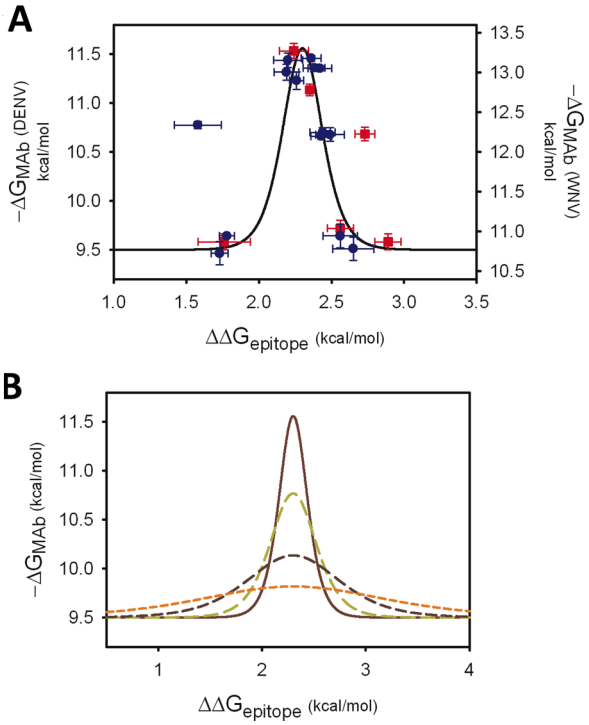

Figure 6. Thermodynamic mechanism in antibody neutralization resistance. (A) The correlation between thermodynamic coupling and binding energy to MAbs follows a peaked function. The values for this figure were obtained by averaging the thermodynamic coupling of the residues in the ED3s that reside in the BC loop for WNV (red symbols) or in the FG loop for DENV-2 (blue symbols). The error bars correspond to the standard deviation of the mean. The binding energies were obtained from Table 1. The black line is a fit of the response of a Boltzmann equilibrium process (eq 7 in Methods). (B) Changes in the response of the Boltzmann fit using decreasing cooperativity values (C = 6.5 in brown, C = 4.0 in green, C = 2.0 in dark brown, and C = 1 in orange).

of epitope residues (i.e., $\Delta\Delta G^{\text{mutant}}_{\text{epitope}} > \Delta\Delta G^{\text{wild-type}}_{\text{epitope}}$ or $\Delta\Delta G^{\text{mutant}}_{\text{epitope}} < \Delta\Delta G^{\text{wild-type}}_{\text{epitope}}$). The conserved effect of mutations in both ED3s suggests similar thermodynamic principles in the mechanism of evasion of antibody-mediated neutralization.

The simplest model that describes the peaked function shown in Figure 6 is the response of a Boltzmann (equilibrium) process between two thermodynamic states (eq 7 in Methods). Often in biophysics, a Boltzmann process is described for folded/unfolded, bound/unbound, or active/inactive transitions in a protein. In this study, however, the Boltzmann process represents a transition between low and high thermodynamic coupling states in the epitope of the ED3s. We interpret these thermodynamic coupling states as states of lower or higher fluctuations in the epitope relative to wild-type. By using eq 7 to fit the data in Figure 6A, we determined the midpoint of the transition (x_o = 2.3 kcal/mol) and a cooperativity factor, C, that describes the sharpness of the transition between the two states.[31−33] We obtained a value of C = 6.5, which reflects a sharp transition between states. The high degree of cooperativity implies that mutations that generate small changes in the thermodynamic coupling of the epitope result in a large reduction in the binding energy to a mAb. This is clearly seen in Figure 6A wherein changes in the thermodynamic coupling of the epitope as small as ±0.3 kcal/mol result in a ∼ 1−2 kcal/mol change in binding energy (equivalent to ∼10- and 100-fold decrease in mAb binding affinity).

Balance between Antigenic Variation and Viral Fitness: A Thermodynamic Perspective. To illustrate the biological relevance of a high degree of cooperativity characterizing the transition between thermodynamic coupling states, we systematically reduced C in eq 7 and recorded the changes in the shape of the peaked function observed in Figure 6A. When we reduced the value of C from 6.5 to 1, the height of the peaked function was significantly reduced (Figure 6B). This decrease in height implies that even if a mutation in ED3 generates a large change in the thermodynamic coupling of the epitope, the reduction in the mAb binding affinity will be very small. We also observed that the peaked function broadens as the value of C decreases. This broadening effect indicates that a mutation in ED3 loses efficacy in reducing mAb binding affinity even for large changes in thermodynamic coupling. In fact, for a change of ±0.3 kcal/mol in the thermodynamic coupling and a C = 2, the reduction in mAb binding affinity is only 25%. When C = 1, the expected change in mAb binding affinity is negligible. A phenotype that evades neutralization in WNV and DENV-2 is clearly observed when the mAb binding affinity is reduced 10-fold or more relative to WT. In order to decrease the mAb binding affinity 10-fold when C = 2, the change in thermodynamic coupling in the epitope needs to be as high as 1.5−2.0 kcal/mol. Thermodynamic perturbations of 1.5−2.0 kcal/mol will likely lead to global protein unfolding and render the viral particle nonviable.

Our analysis is logical from a biological point of view because mutations that result in severe changes in the stability of the protein antigen will be selected against. Instead, mutations that generate small changes in the thermodynamic coupling of residues in the epitope would be evolutionarily advantageous and provide the virus with an advantage over neutralizing antibodies without jeopardizing the structural integrity, fold, global stability of the protein antigen, or viability of the infectious virion. Because of the fundamental thermodynamic nature of our analysis, we foresee that the strategy to generate resistance to antibody binding described here may be applicable to other pathogens.

Role of Protein Ensembles in Antibody-Mediated Neutralization. Previous studies have proposed that epitopes are predominantly located in flexible regions of a protein antigen.[37−41] However, no quantitative thermodynamic mechanism was proposed for such observations. Our studies, however, provide a thermodynamic foundation for the role of protein flexibility in escape mutants. We found that resistant mutations increase or decrease the flexibility of the epitope by tuning up or down the degree of thermodynamic coupling between the site of mutation and the epitope. The modulation of thermodynamic coupling may occur via linear effects (mutations in the epitope) or by conformational effects (mutations in neighboring structures of the epitope). These long-range mutational effects probably originate in the redistribution of conformational states within the ensemble of the ED3s[42] and not through a direct mechanical pathway that evokes a static view of proteins. We envision that long-range interactions between residues residing in the epitopes and other amino acids may provide additional mutation sites in the virus to increase antigenic variations that allow the virus to go undetected by the host immune system.

Altogether, the application of an ensemble-based description of protein fluctuations quantitatively explains the effect of

mutations in evasion of antibody neutralization. Ensemble-based descriptions of the equilibrium have been successfully used to describe the mechanism of allosteric regulation in other protein systems (i.e., DHFR and cAMP receptor protein). Thus, changes in the subpopulations of the native state ensemble (due to mutation, ligand binding, or protein−protein interactions) seem to be a general strategy that nature uses to regulate biological function, including escape from antibody binding.

CONCLUSIONS

The parallel observations for WNV and DENV-2 allowed us to establish a unified mechanism of antibody-mediated neutralization for these two viruses. This mechanism correlates subtle changes in the conformational fluctuations in the epitope (described as thermodynamic coupling) and large defects in antibody binding affinity. The consequence of such correlation is that the virus is efficiently undetected by neutralizing antibodies without global unfolding of the viral protein. Viruses have evolved many strategies to survive neutralizing antibodies, including the disruption of interaction surfaces between the epitope and the antibody (steric hindrance).[43−45] Here, we describe the role of protein conformational fluctuations and how mutations inside or outside the epitope lead to evasion to antibody neutralization (Figure 7).

Antibody neutralization is a central component of the immune response against viruses, as antibodies reduce viral infectivity by preventing cell entry and tissue dissemination.[2,20,46−48] A large effort is being invested in identifying epitopes in proteins from these and other flaviviruses.[1−7,9,19,23,24,46,49] Correctly identifying the epitopes is very important, since it will allow the development of new and efficient therapies (i.e., therapeutic antibodies),[2,7,12,17,20,50] or the identification of target sites for small molecules to bind and inactivate viral proteins. Without *a priori* information on the epitopes, our studies revealed a previously unidentified relationship between mutational susceptibility of the ensemble and epitope location. Thus, an important and fundamental question arises: *What is an epitope?* From a functional perspective, an epitope has been identified by mutations that decrease antibody-binding affinity and generate a neutralization-resistant phenotype in a virus. From a structural point of view, epitopes have been assigned as residues that are part of an interaction surface between the protein antigen and the antibody. In this study, we add a dimension to the identification of an epitope based on the fundamental thermodynamic property of correlated fluctuations in the protein ensemble. We propose that the combination of functional data, high-resolution structures, and thermodynamic information should allow a more accurate identification of the key residues responsible for the generation of evasion to antibody-mediated neutralization of viruses or other pathogens.

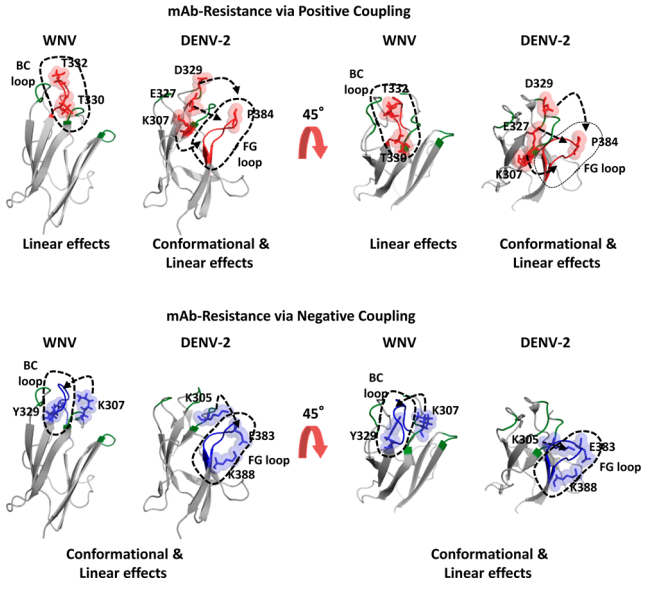

Figure 7. Viral strategies in antibody neutralization resistance involve changes in protein conformational fluctuations. Structure of the ED3 from WNV bound to a monoclonal antibody.[12] A static view of the mechanism of antibody resistance involves steric hindrance of tight antibody−antigen interactions due to mutations in the epitope (i.e., at position T332, green arrowhead). Alternatively, but not exclusively, mutations in the viral epitope (red arrowhead) may lead to changes in the conformational dynamics of the protein antigen to prevent antibody binding. Moreover, we found that mutations not located in the primary epitope (the BC loop in WNV) that are thermodynamically coupled can also lead to antibody neutralization resistance via conformational effects (black arrowhead). In this figure, the BC loop is rendered in red color.

AUTHOR INFORMATION

Corresponding Authors

jclee@utmb.edu

ram279@georgetown.edu

Present Addresses

[#]R.A.M.: Department of Chemistry, Georgetown University, Washington, DC.20057.

[§]T.L.: Sequenom Inc., 3595 John Hopkins Court, San Diego, CA 92121.

[▽]V.J.H.: Department of Biology, Johns Hopkins University, 3400 N. Charles Street Baltimore, MD 21218-2685.

Notes

The authors declare no competing financial interest.

ACKNOWLEDGMENTS

Supported by NIH Grant GM 77551 and the Robert A. Welch Foundation to J.C.L. and a grant from Pediatric Dengue Vaccine Initiative to A.D.T.B. and J.C.L. We thank Drs. Maria Fe Lanfranco Gallofre, Heather M. Landers, and Karon P. Cassidy for their valuable assistance in the preparation of the manuscript.

REFERENCES

(1) Beasley, D. W.; Barrett, A. D. *J. Virol.* **2002**, *76*, 13097.

(2) Buckley, A.; Gould, E. A. *J. Gen. Virol.* **1985**, *66* (Pt 12), 2523.

(3) Cecilia, D.; Gadkari, D. A.; Kedarnath, N.; Ghosh, S. N. *J. Gen. Virol.* **1988**, *69* (Pt 11), 2741.

(4) Cecilia, D.; Gould, E. A. *Virology* **1991**, *181*, 70.

(5) Gromowski, G. D.; Barrett, N. D.; Barrett, A. D. *J. Virol.* **2008**, *82*, 8828.

(6) Guirakhoo, F.; Heinz, F. X.; Kunz, C. *Virology* **1989**, *169*, 90.

(7) Matsui, K.; Gromowski, G. D.; Li, L.; Schuh, A. J.; Lee, J. C.; Barrett, A. D. *Virology* **2009**, *384*, 16.

(8) Sukupolvi-Petty, S.; Austin, S. K.; Purtha, W. E.; Oliphant, T.; Nybakken, G. E.; Schlesinger, J. J.; Roehrig, J. T.; Gromowski, G. D.; Barrett, A. D.; Fremont, D. H.; Diamond, M. S. *J. Virol.* **2007**, *81*, 12816.

(9) Zhang, S.; Bovshik, E. I.; Maillard, R.; Gromowski, G. D.; Volk, D. E.; Schein, C. H.; Huang, C. Y.; Gorenstein, D. G.; Lee, J. C.; Barrett, A. D.; Beasley, D. W. *Virology* **2010**, *403*, 85.

(10) Mukhopadhyay, S.; Kim, B. S.; Chipman, P. R.; Rossmann, M. G.; Kuhn, R. J. *Science* **2003**, *302*, 248.
(11) Yu, I. M.; Zhang, W.; Holdaway, H. A.; Li, L.; Kostyuchenko, V. A.; Chipman, P. R.; Kuhn, R. J.; Rossmann, M. G.; Chen, J. *Science* **2008**, *319*, 1834.
(12) Nybakken, G. E.; Oliphant, T.; Johnson, S.; Burke, S.; Diamond, M. S.; Fremont, D. H. *Nature* **2005**, *437*, 764.
(13) Volk, D. E.; Beasley, D. W.; Kallick, D. A.; Holbrook, M. R.; Barrett, A. D.; Gorenstein, D. G. *J. Biol. Chem.* **2004**, *279*, 38755.
(14) Volk, D. E.; Chavez, L.; Beasley, D. W.; Barrett, A. D.; Holbrook, M. R.; Gorenstein, D. G. *Virology* **2006**, *351*, 188.
(15) Volk, D. E.; Lee, Y. C.; Li, X.; Thiviyanathan, V.; Gromowski, G. D.; Li, L.; Lamb, A. R.; Beasley, D. W.; Barrett, A. D.; Gorenstein, D. G. *Virology* **2007**, *364*, 147.
(16) Volk, D. E.; May, F. J.; Gandham, S. H.; Anderson, A.; Von Lindern, J. J.; Beasley, D. W.; Barrett, A. D.; Gorenstein, D. G. *Virology* **2009**, *394*, 12.
(17) Midgley, C. M.; Flanagan, A.; Tran, H. B.; Dejnirattisai, W.; Chawansuntati, K.; Jumnainsong, A.; Wongwiwat, W.; Duangchinda, T.; Mongkolsapaya, J.; Grimes, J. M.; Screaton, G. R. *J. Immunol.* **2012**, *188*, 4971.
(18) Cockburn, J. J.; Navarro Sanchez, M. E.; Fretes, N.; Urvoas, A.; Staropoli, I.; Kikuti, C. M.; Coffey, L. L.; Arenzana Seisdedos, F.; Bedouelle, H.; Rey, F. A. *Structure* **2012**, *20*, 303.
(19) Li, L.; Barrett, A. D.; Beasley, D. W. *Virology* **2005**, *335*, 99.
(20) Oliphant, T.; Engle, M.; Nybakken, G. E.; Doane, C.; Johnson, S.; Huang, L.; Gorlatov, S.; Mehlhop, E.; Marri, A.; Chung, K. M.; Ebel, G. D.; Kramer, L. D.; Fremont, D. H.; Diamond, M. S. *Nat. Med.* **2005**, *11*, 522.
(21) Maillard, R. A.; Jordan, M.; Beasley, D. W.; Barrett, A. D.; Lee, J. C. *J. Biol. Chem.* **2008**, *283*, 613.
(22) Zhang, S.; Vogt, M. R.; Oliphant, T.; Engle, M.; Bovshik, E. I.; Diamond, M. S.; Beasley, D. W. *J. Infect. Dis.* **2009**, *200*, 202.
(23) Lin, C. W.; Wu, S. C. *J. Virol.* **2003**, *77*, 2600.
(24) Gromowski, G. D.; Barrett, A. D. *Virology* **2007**, *366*, 349.
(25) Wrabl, J. O.; Gu, J.; Liu, T.; Schrank, T. P.; Whitten, S. T.; Hilser, V. J. *Biophys. Chem.* **2011**, *159*, 129.
(26) Hilser, V. J.; Dowdy, D.; Oas, T. G.; Freire, E. *Proc. Natl. Acad. Sci. U. S. A.* **1998**, *95*, 9903.
(27) Hilser, V. J.; Freire, E. *J. Mol. Biol.* **1996**, *262*, 756.
(28) Liu, T.; Whitten, S. T.; Hilser, V. J. *Proteins* **2006**, *62*, 728.
(29) Liu, T.; Whitten, S. T.; Hilser, V. J. *Proc. Natl. Acad. Sci. U. S. A.* **2007**, *104*, 4347.
(30) Whitten, S. T.; Garcia-Moreno, B. E.; Hilser, V. J. *Methods Cell Biol.* **2008**, *84*, 871.
(31) Bai, Y.; Sosnick, T. R.; Mayne, L.; Englander, S. W. *Science* **1995**, *269*, 192.
(32) Planells-Cases, R.; Ferrer-Montiel, A. V.; Patten, C. D.; Montal, M. *Proc. Natl. Acad. Sci. U. S. A.* **1995**, *92*, 9422.
(33) Tytgat, J.; Hess, P. *Nature* **1992**, *359*, 420.
(34) Oliphant, T.; Nybakken, G. E.; Austin, S. K.; Xu, Q.; Bramson, J.; Loeb, M.; Throsby, M.; Fremont, D. H.; Pierson, T. C.; Diamond, M. S. *J. Virol.* **2007**, *81*, 11828.
(35) Gromowski, G. D.; Roehrig, J. T.; Diamond, M. S.; Lee, J. C.; Pitcher, T. J.; Barrett, A. D. *Virology* **2010**, *407*, 237.
(36) Hiramatsu, K.; Tadano, M.; Men, R.; Lai, C. J. *Virology* **1996**, *224*, 437.
(37) Adhikary, R.; Yu, W.; Oda, M.; Zimmermann, J.; Romesberg, F. E. *J. Biol. Chem.* **2012**, *287*, 27139.
(38) Fieser, T. M.; Tainer, J. A.; Geysen, H. M.; Houghten, R. A.; Lerner, R. A. *Proc. Natl. Acad. Sci. U. S. A.* **1987**, *84*, 8568.
(39) Jimenez, R.; Salazar, G.; Baldridge, K. K.; Romesberg, F. E. *Proc. Natl. Acad. Sci. U. S. A.* **2003**, *100*, 92.
(40) Jimenez, R.; Salazar, G.; Yin, J.; Joo, T.; Romesberg, F. E. *Proc. Natl. Acad. Sci. U. S. A.* **2004**, *101*, 3803.
(41) Westhof, E.; Altschuh, D.; Moras, D.; Bloomer, A. C.; Mondragon, A.; Klug, A.; Van Regenmortel, M. H. *Nature* **1984**, *311*, 123.
(42) Pan, H.; Lee, J. C.; Hilser, V. J. *Proc. Natl. Acad. Sci. U. S. A.* **2000**, *97*, 12020.
(43) Davies, D. R.; Cohen, G. H. *Proc. Natl. Acad. Sci. U. S. A.* **1996**, *93*, 7.
(44) Davies, D. R.; Sheriff, S.; Padlan, E. A. *J. Biol. Chem.* **1988**, *263*, 10541.
(45) Braden, B. C.; Poljak, R. J. *FASEB J.* **1995**, *9*, 9.
(46) Brien, J. D.; Austin, S. K.; Sukupolvi-Petty, S.; O'Brien, K. M.; Johnson, S.; Fremont, D. H.; Diamond, M. S. *J. Virol.* **2010**, *84*, 10630.
(47) Shrestha, B.; Brien, J. D.; Sukupolvi-Petty, S.; Austin, S. K.; Edeling, M. A.; Kim, T.; O'Brien, K. M.; Nelson, C. A.; Johnson, S.; Fremont, D. H.; Diamond, M. S. *PLoS Pathog.* **2010**, *6*, No. e1000823.
(48) Sukupolvi-Petty, S.; Austin, S. K.; Engle, M.; Brien, J. D.; Dowd, K. A.; Williams, K. L.; Johnson, S.; Rico-Hesse, R.; Harris, E.; Pierson, T. C.; Fremont, D. H.; Diamond, M. S. *J. Virol.* **2010**, *84*, 9227.
(49) Holzmann, H.; Stiasny, K.; Ecker, M.; Kunz, C.; Heinz, F. X. *J. Gen. Virol.* **1997**, *78* (Pt 1), 31.
(50) Sundberg, E. J.; Mariuzza, R. A. *Adv. Protein Chem.* **2002**, *61*, 119.
(51) Pitcher, T. J.; Gromowski, G. D.; Beasley, D. W.; Barrett, A. D. *Virology* **2012**, *422*, 386.